

# Polypyrrole Electrodeposition on Ti6Al7Nb Alloy in Aqueous and Non-aqueous Solutions

VASILICA MIHAELA MINDROIU<sup>1</sup>, CRISTIAN PIRVU<sup>1\*</sup>, SIMONA POPESCU<sup>1</sup>, IOANA DEMETRESCU<sup>1</sup>

<sup>1</sup> University Politehnica of Bucharest, Faculty of Applied Chemistry and Materials Science, 1-7 Polizu Str., 011061, Bucharest, Romania

*Polypyrrole were synthesized by electrochemical methods both in aqueous and non-aqueous media on Ti6Al7Nb alloy as substrate. The potentiodynamic, potentiostatic and galvanostatic procedures were used for polypyrrole electrodeposition. The surface analysis of the titanium alloy/polypyrrole surface was performed by atomic force microscopy showed that the film obtained in acetonitrile was more adherent on the surface comparing with that obtained in aqueous solution. This different behaviour is probably due to the lower adherence of polypyrrole on oxidized surfaces existing in aqueous solutions.*

*Keywords: titanium alloy, polypyrrole, electropolymerization*

Modifications of solid inorganic surfaces are often used to change properties such as biocompatibility, wetting, adhesion and friction. Depositions of polymer layers are recognized to play an important role, especially in printing, coating, food packaging, biomedical and aerospace applications. There are numerous ways of modifying inorganic substrates with polymer, by chemical, electrochemical [1, 2] as well as by physical means (e.g. spin coating, physisorption) [3].

Titanium alloys have the advantageous combination of low density, high mechanical resistance and an effective corrosion inhibition due to the ultra-thin (about 5 nm) and uniformly covering oxide layer. The association of these properties has made Ti6Al7Nb material of choice for bone repairs (prostheses, implants) as well as for pacemakers and pumps.

However, corroding actions by the biological environment (blood, saliva) have been pointed out and failures of integration of Ti-based materials have also been reported [4]. Polypyrrole films deposited on Ti6Al7Nb substrates could be used to graft biologically active molecules which accelerate the process of osseointegration [5] and protect the surface of the substrate from corrosion. Polypyrrole has also been used as an active component of bilayer or multilayer strips in artificial muscles and micro machined structures [6–8].

Conducting polymers can be prepared *via* chemical or electrochemical polymerization [9]. The latter is generally preferred because it provides a better control of film thickness and morphology and cleaner polymers when compared to chemical oxidation. Films of electronically conducting polymers are generally deposited onto a supporting electrode surface by anodic oxidation (electropolymerization) of the corresponding monomer in the presence of an electrolyte solution. Different electrochemical procedures can be used including potentiostatic (constant-potential), galvanostatic (constant current) and potentiodynamic (potential scanning *i.e.* cyclic voltammetry) methods [10]. Electrical conductivity is achieved in the film of conducting polymer by oxidation (p-doping) or reduction (n-doping), followed by the insertion

of anionic or cationic species, respectively [10]. Due to the double bond alternation in the conjugated polymer backbone, the charged species formed upon doping are able to move along the carbon chain (delocalization) allowing electron transport and thus giving an electronically conductive material [11].

In an electrochemical polymerization, the monomer, dissolved in an appropriate solvent containing the desired anionic doping salt, is oxidized at the surface of an electrode by application of an anodic potential (oxidation). The choice of the solvent and electrolyte is of particular importance in electrochemistry since both solvent and electrolyte should be stable at the oxidation potential of the monomer and provide an ionically conductive medium. Organic solvents like acetonitrile or propylene carbonate have very large potential windows [12], and high relative permittivities, which allow a good dissociation of the electrolyte substances and thus a good ionic conductivity. Since pyrrole has a relatively low oxidation potential, [13] electro-polymerization can be carried out in aqueous electrolytes which is not possible for thiophene or benzene.

In this paper, we present results about the deposition of polypyrrole (PPy) at Ti6Al7Nb electrode surface by three procedures: potentiostatic techniques, galvanostatic techniques and cycle voltammetry using 0.1 M LiClO<sub>4</sub> aqueous and non-aqueous monomer solutions with acetonitrile (ACN) as solvent. From all electrochemical techniques a polymer film was also obtained; however in aqueous medium the adhesion of polypyrrole to Ti6Al7Nb electrode surface is lower than that obtained in acetonitrile solution.

## Experimental part

Pyrrole (Py) monomer was purchased from Aldrich, distilled and stored in the dark at -20°C prior to use. Lithium perchlorate (≥99%, Aldrich) was dissolved in a concentration of 0.1 M in distilled water and acetonitrile (99%, Aldrich). The electrodes were constructed from Ti-6Al-7Nb alloy with composition given in table 1; all experiments were carried out on disk-shaped samples (1

Table 1  
CHEMICAL COMPOSITION OF THE Ti-6Al-7Nb ALLOY

Element	Ti	Al	Nb	Fe	H	N	O	C
Percentages (wt%)	rest	5.88	6.65	0.3	0.0121	0.05	0.2	0.1

\* email address: c\_pirvu@chim.upb.ro; Tel.: +40 21 402 3930

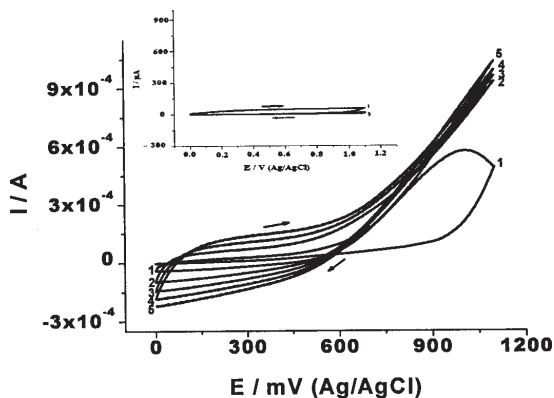


Fig. 1. Cyclic voltammograms obtained on Ti6Al7Nb electrode in 0.1 mol L<sup>-1</sup> pyrrole in 0.1 mol L<sup>-1</sup> LiClO<sub>4</sub> aqueous solution; the inset presents cyclic voltammograms obtained in 0.1 mol L<sup>-1</sup> LiClO<sub>4</sub> aqueous solution, 5 cycles between 0 V and 1.1 V at 50 mV/s

cm diameter, 2 cm thickness). Their surface was polished with 1200 silicon carbide paper and rinsed well with distilled water before performing the electrodeposition experiments.

The electrolytes used in this paper were aqueous and acetonitril solutions of 0.1 mol L<sup>-1</sup> Py; a 0.1 mol L<sup>-1</sup> LiClO<sub>4</sub> solution was used as support electrolyte.

The electrochemical measurements were performed using a one compartment cell with three electrodes: working electrode, platinum counter-electrode and Ag/AgCl, KCl reference electrode, connected to Autolab PGSTAT 302 N potentiostat with general-purpose electrochemical system software.

The surface topography and morphologies of polypyrrole films polymerised under identical conditions from aqueous and acetonitril solutions were studied with Atomic Force Microscopy (AFM).

## Results and discussions

### Electropolymerization of pyrrole on Ti6Al7Nb electrode from aqueous solution

#### Potentiodynamic polymerization

The potentiodynamic polymerization of pyrrole was carried out in 0.1 M LiClO<sub>4</sub> aqueous solution in the presence of 0.1 M pyrrole (Fig. 1). It can be seen clearly that all CVs show similar characteristics to those of other conducting polymers, indicating that the polymerisation proceeded easily even at low monomer concentrations.

On the first CV cycle the current densities on the reverse scan are higher than that on the forward scan (in the region of 0.7–1.1V). The formation of this loop can be explained as characteristics of a nucleation process [14–18]. The increase of the current densities with increasing cycle number of the potential scans implies that the amount of the polymer on the electrode increased cycle by cycle. The films obtained are black and homogeneous to the electrode surface.

The successive sweeps show a capacitive behaviour on the potential range 0–600 mV, which increases with the cycle number of the potential scan. After six voltammetric cycles the difference between anodic and cathodic current on this potential range reached around 300 mV.

#### Potentiostatic polymerization

The electrosynthesis of PPy films on Ti6Al7Nb electrode can be also performed by the potentiostatic technique, in one potential step, by applying the potential of 0.9 V vs. Ag/AgCl.

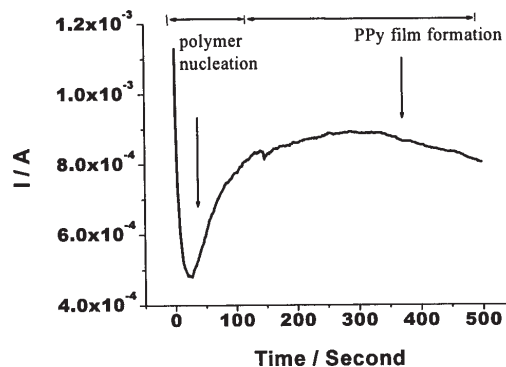


Fig. 2. Chronoamperometric curve during potentiostatic electrodeposition of 0.1 mol L<sup>-1</sup> pyrrole in 0.1 mol L<sup>-1</sup> LiClO<sub>4</sub> aqueous solution on a Ti6Al7Nb electrode at the applied potential of 0.9 V.

The current transient obtained for a typical potentiostatic PPy electrodeposition is presented in figure 2. The chronoamperogram can be divided into two stages. At the beginning, the current density decays during the polymer nucleation. In the second stage the current density increases linearly with the time. This last behaviour, without overlap, can be due to the growth of either independent nuclei alone or a combination of this process with simultaneous increase in number of nuclei. The total charge used for potentiostatic polymerization of pyrrole at 0.9 V was 406 mC for our electrode

#### Galvanostatic polymerization

Figure 3 shows the growth of a PPy film on Ti6Al7Nb electrode by galvanostatic electrodeposition at the applied current of 90 μA. Simultaneously to electropolymerisation other processes, such as metal oxidation and passivation, take also place and compete during formation of the PPy films. According to [19], the monomer oxidation and polymerisation process are favoured by high current densities. Other researches [20] state that the initial linear potential increase during the current pulse indicates a formation of an oxide layer on titanium alloy electrode. When the dielectric barrier is broken, the potential remains practically constant during the development of a conducting coating; in figure 3 this phase is reached in a few seconds.

The polymerization potential plateau is stabilized at 0.65 V value which is similar with the value of the starting monomer oxidation potential from the cyclic voltammogram.

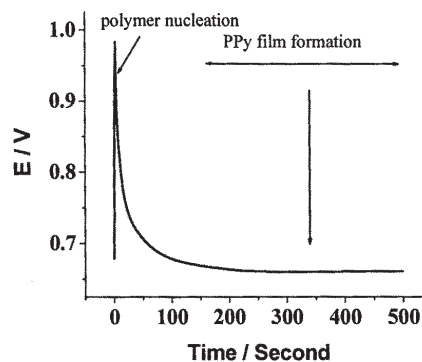


Fig. 3. Electropolymerisation by galvanostatic electrodeposition of 0.1 mol L<sup>-1</sup> pyrrole in 0.1 mol L<sup>-1</sup> LiClO<sub>4</sub> aqueous solution on a Ti6Al7Nb electrode at the applied current of 90 μA

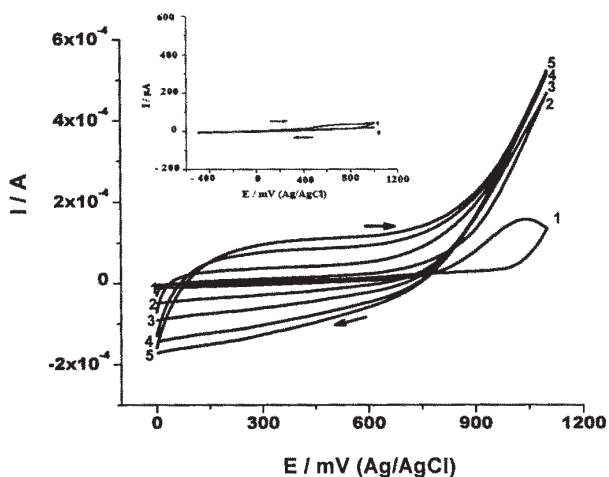


Fig. 4. Cyclic voltammograms obtained on Ti6Al7Nb electrode in 0.1 mol L<sup>-1</sup> pyrrole and 0.1 mol L<sup>-1</sup> LiClO<sub>4</sub> acetonitrile solution; the inset presents cyclic voltammograms obtained in 0.1 mol L<sup>-1</sup> LiClO<sub>4</sub> acetonitrile solution, 5 cycles between 0 V and 1.1 V at 50 mV/s

#### Electropolymerization of pyrrole on Ti6Al7Nb electrode from acetonitrile solution

##### Potentiodynamic polymerization

Figure 4 shows the cyclic voltammograms obtained on Ti6Al7Nb electrode in 0.1 mol L<sup>-1</sup> LiClO<sub>4</sub> acetonitrile monomer solution. The voltammograms present a quasi similar behaviour with those observed on the polymerization in aqueous solution the single difference being in the oxidation potential of monomer which is more positive in acetonitrile electrolyte, 0.8 V.

Also, the successive sweeps show a capacitive behaviour on the larger potential range of 0-800 mV which increases with the cycle number of the potential. After six voltammetric cycles the difference between anodic and cathodic current on this potential range was around 300 mV.

The anodic charge used for potentiodynamic polymerization on every cycle both in aqueous and organic electrolyte is presented in figure 5. In order to avoid the overlapping of the polymerization charge and the oxidation of titanium alloy substrate charge, the last one was subtracted from the total charge.

Higher values of the anodic charge on the polymerization in aqueous solution can be observed for all scans. The charge difference between aqueous and organic electrolyte polymerization increases with the number of potential cycles suggesting that a larger amount of polymer is formed in aqueous solution.

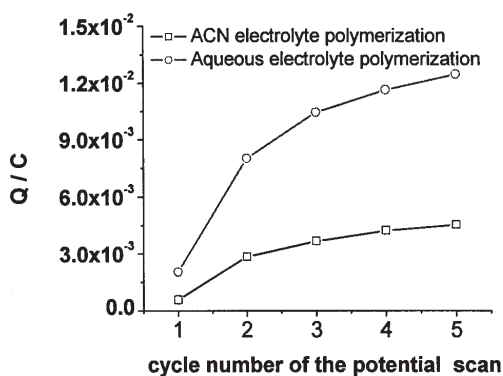


Fig. 5. Charge of anodic branch vs. cycle number of the potential scan, for two investigated solutions

##### Potentiostatic polymerization

The electrosynthesis of PPy films on Ti6Al7Nb electrode were also performed by the potentiostatic technique, in one potential step, by applying the potential of 0.9 V vs. Ag/AgCl.

The current transient obtained for a typical potentiostatic PPy electrodeposition presented in figure 6 is quite different comparing with that obtained in aqueous solution (fig. 2). The chronoamperograms can be also divided into two stages. At the beginning, the current density increases during the polymer nucleation but in the second stage the amplitude of current density plateau is ten times lower than that obtained in aqueous solution.

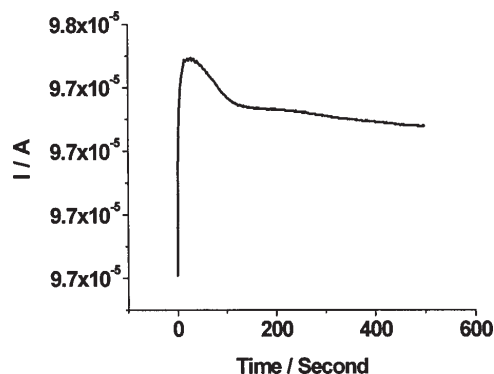


Fig. 6. Chronoamperometric curves during potentiostatic electrodeposition of 0.1 mol L<sup>-1</sup> pyrrole in 0.1 mol L<sup>-1</sup> LiClO<sub>4</sub> acetonitrile solution on a Ti6Al7Nb electrode at the applied potential of 0.9 V

The total charge used for potentiostatic polymerization of pyrrole in acetonitrile solution was 48 mC for the used Ti electrode.

The film obtained in acetonitrile is more adherent on the titanium alloy surface comparing with that obtained in aqueous solution, probably to the existence of an oxidized surface in last medium.

##### Galvanostatic polymerization

Figure 7 shows the growth of a PPy film on Ti6Al7Nb electrode by galvanostatic electrodeposition at the applied current of 90 μA in acetonitrile solution. The start potential step is about 550 mV and then the potential moves to less positive potentials.

The polymerization potential plateau is stabilized at 0.8 V, a value which is also similar with the value of the starting monomer oxidation potential from the cyclic voltammogram recorded in acetonitrile solution.

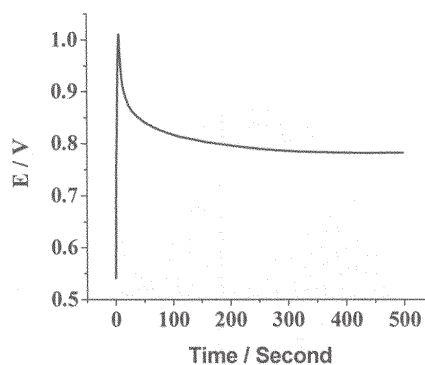


Fig. 7. Electropolymerisation by galvanostatic electrodeposition of 0.1 mol L<sup>-1</sup> pyrrole in 0.1 mol L<sup>-1</sup> LiClO<sub>4</sub> acetonitrile solution on a Ti6Al7Nb electrode at the applied current of 90 μA

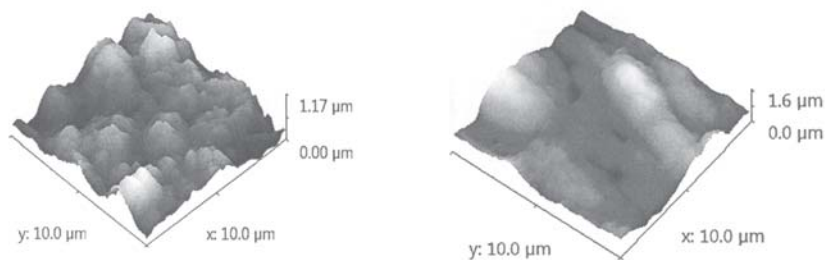


Fig. 8. Three-dimensional images of 10  $\mu\text{m}$  scans for potentiostatic (0.9 V) polymerized polypyrrole in acetonitrile (a) and aqueous (b) electrolytes

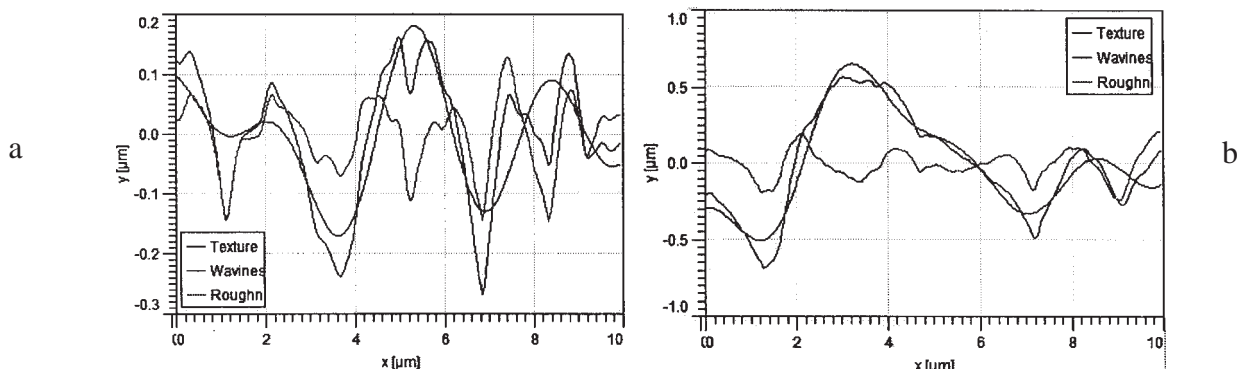


Fig. 9. Texture, waviness and roughness of the surface for potentiostatic (0.9 V) polymerized polypyrrole in acetonitrile (a) and aqueous (b) electrolytes

**Table 2**  
THE ROUGHNESS FOR THE SURFACE OF Ti ALLOY/  
POLYPYRROLE ELECTRODEPOSITED IN AQUEOUS AND  
NON-AQUEOUS SOLUTION

Electropolymerization	Ra ( $\mu\text{m}$ )	Rms ( $\mu\text{m}$ )
In ACN electrolyte	0.145	0.189
In aqueous electrolyte	0.243	0.304

#### Structural analysis of PPy films

In order to investigate the surface topography of polypyrrole modified surfaces the contact mode AFM microscopy was used.

Figure 8 shows examples of three-dimensional images of 10x10  $\mu\text{m}$  scans for potentiostatic (0.9 V) polymerized polypyrrole in acetonitrile (a) and aqueous (b) electrolytes.

The surface of potentiostatically deposited polypyrrole in acetonitrile electrolyte is characterised by formation of grains of about 2-3  $\mu\text{m}$  dimensions which increase on a regulated polypyrrole surface. From AFM images we obtained the roughness data presented in table 2.

Ra is the roughness average, and Rms represents the root mean square parameter.

The waviness of the surface for potentiostatically deposited polypyrrole on titanium in aqueous solution shows the presence of the large grain with around 5-6  $\mu\text{m}$  dimensions. A comparison of data obtained in both electrolytic media is made in figure 9.

It is evident that the roughness is higher for the surface of polypyrrole electrodeposited in aqueous solution.

#### Molecular structure of PPy films

The Fourier transform infrared (FT-IR) spectroscopic analysis for polypyrrole films electrodeposited both in aqueous and organic electrolyte was done by Perkin Elmer FTIR spectrophotometer 100 using diamond ATR technique. The obtained spectra are presented in figure 10.

Both FT-IR absorption spectra of PPy presents a quasi similar aspect. The NH stretching band of pyrrole ring appears at 3500  $\text{cm}^{-1}$ . The weak band at 2900  $\text{cm}^{-1}$  is due to C-H stretching. The other bands also show the

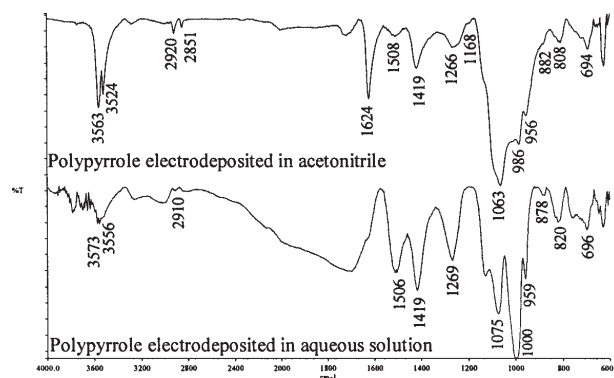


Fig. 10. The FT-IR spectrum of polypyrrole films electrodeposited both in aqueous and organic electrolyte.

characteristic polypyrrole absorption at 1600-1100  $\text{cm}^{-1}$ . An absorption at 1624  $\text{cm}^{-1}$  was assigned to the C=C ring stretching of pyrrole. The C-N ring stretching band of pyrrole ring occurs at 1419  $\text{cm}^{-1}$ . The peak at 1168  $\text{cm}^{-1}$  is due to C-C stretching [21].

The band at 1506  $\text{cm}^{-1}$  (2, 5 substituted polypyrrole) and 1419  $\text{cm}^{-1}$  may be assigned to typical polypyrrole ring vibrations.

The IR peak observed at 889  $\text{cm}^{-1}$  may be assigned to the =C-H out of plane vibration indicating the polymerization of pyrrole [22].

#### Conclusions

By comparing polypyrrole films synthesized by electrochemical procedures in both aqueous and non-aqueous media on Ti6Al7Nb alloy, we noticed that the film obtained in acetonitrile is more adherent on the Ti surface. This behaviour may be probably due to the lower adherence of polypyrrole on oxidized surfaces existing in aqueous solutions.

The surface analysis by AFM technique of potentiostatically deposited polypyrrole on titanium alloy surface shows the formation of grains of about 2-3  $\mu\text{m}$  in ACN electrolyte and 5-6  $\mu\text{m}$  in aqueous solution.

The FT-IR absorption spectra of PPy present a quasi similar aspect suggesting the same structure of polymeric film.

*Acknowledgements. The authors gratefully acknowledge the support of the Romanian CNCSIS Program PCCE, Project no. 248/2009.*

## References

1. PIRVU, C., STANCU, R., SOVAR, M., Rev. Chim.(Bucharest), **58**, no. 10, 2007, p. 861
2. MAN, I., PIRVU, C., DEMETRESCU, I., Rev. Chim.(BUcharest), **59**, no. 6, 2008, p. 615
3. LUZINOV, I., JULTHONGPIPUT, D., LIEBMANN-VINSON, A., CRAGGER, T., FOSTER, M.D., TSUKRUK, V.V., Langmuir, **16**, 2000, p.504
4. MINDROIU, M., CICEK, E., MICULESCU, F., DEMETRESCU, I., Rev.Chim.(Bucharest), **58**,no. 9, 2007, p. 898
5. POPESCU, B., VASILESCU, E., DROB, P., VASILESCU, C., ISTRATESCU, M., Rev. Chim.(BUcharest), **56**, no. 10, 2005, p. 999
6. PEI, Q., INGANAS, O., Adv. Mater., **4**, (4), 1992, p. 277
7. BAUGHMAN, R.H., Synth. Met., **78**, 1996, p. 339
8. SMELA, E., INGANAS, O., LUNDSTROM, I., Science, **268**, 1995, p. 1735
9. HEINZE, J., Top. Curr. Chem., **152**, 1990, p. 2
10. DOBLHOFER K., RAJESHWAR, K., Handbook of Conducting Polymers, 2<sup>nd</sup> Edn., ed. T. A. Skotheim, R. L. Elsenbaumer and J. R. Reynolds, Marcel Dekker, New York, 1998, p.531
11. LYONS, M.E.G., Advances in Chemical Physics, Polymeric Systems, I. Prigogine and S. A. Rice, John Wiley & Sons, New York, **94**, 1997, p.297
12. BARD, A.J., FAULKNER, L.R., Electrochemical Methods, Fundamentals and Applications, Eds. John Wiley & Sons, New York, second ed., 2000.
13. RODRIGUEZ, J., GRANDE, H.J., OTERO, T.F., Handbook of Organic Conductive Molecules and Polymers, ed. H. S. Nalwa, John Wiley & Sons, New York, 1997, p. 415
14. DOWNARD, A.J., PLETCHER, D.A., J Electroanal Chem, **206**, 1986, p. 139
15. DOWNARD, A.J., PLETCHER, D.A., J Electroanal Chem, **206**, 1986, p. 147
16. NOFTLE, R.E., PLETCHER, D., J Electroanal Chem, **227**, 1987, 229
17. RANDRIAMHAZAKA, H., NOËL, V., CHEVROT, C., J Electroanal Chem, **472**, 1999, p. 103
18. ZHANG, S., HOU, J., ZHANG, R., XU, J., NIE, G., PU, S., Eur. Polymer J., **42**, 2006, p. 149
19. GUSTAFSSON, H., KVARNSTRÖM, C., IVASKA, A., Thin Solid Films, **517**, 2008, p. 474
20. MARTINS, J.I., COSTA, S.C., BAZZAOU, M., GONÇALVES, G., FORTUNATO, E., MARTINS, R., J. Power Sources, **160**, 2006, p. 1471
21. YEE, L.M., KASSIM, A., EKRAMUL MAHMUD, H.N.M., SHARIF, A.M., HARON, M.J., The Malaysian J. Anal. Sci., **11**, 2007, p. 133
22. VISHNUVARDHAN, T.K., KULKARINI, V.R., BASAVARAJA, C., RAGHAVENDRA, S.C., Bull.Mater.Sci., **29**, 2006, p. 77

Manuscript received: 29.05. 2009